Neoplasma 2023; 70(6): 713–721

doi:10.4149/neo_2023_230711N362

miR-124 delivered by BM-MSCs-derived exosomes targets MCT1 of tumor-infiltrating Treg cells and improves ovarian cancer immunotherapy

Tian GAO#, Yong-Qing LIN#, Hai-Yan YE*, Wu-Mei LIN*

Department of Gynecology, Guangdong Provincial People's Hospital, Guangdong Academy of Medical Sciences, Southern Medical University, Guangzhou, China

**Correspondence: yanzi8174296@163.com; 461099006@qq.com*
#Contributed equally to this work.

Received July 11, 2023 / Accepted November 6, 2023

Metabolic rewiring of tumor cells leads to an enrichment of lactate in the tumor microenvironment (TME). This lactate-rich environment of solid tumors has been reported to support tumor-infiltrating regulatory T (Treg) cells. Therefore, agents that modify the lactate metabolism of Treg cells have therapeutic potential. Monocarboxylate transporter 1 (MCT1), which Treg cells predominantly express, plays an essential role in the metabolism of tumor-infiltrating Treg cells. In this study, we show that miR-124 directly targets MCT1 and reduces lactate uptake, eventually impairing the immune-suppressive capacity of Treg cells. Particularly, exosomal miR-124 derived from bone marrow mesenchymal stromal cells (BM-MSCs) slows tumor growth and increases response to PD-1 blockade therapy. These data indicate a potential treatment strategy for improving immune checkpoint blockade therapy using miR-124-carried BM-MSCs-derived exosomes.

Key words: miR-124; BM-MSC; Treg; exosome; monocarboxylate transporter 1 (MCT1)

microRNAs (miRNAs) are functionally small non-coding RNAs processed from hairpin-containing primary transcripts (pri-miRNA) and are closely involved in the development and progression of cancer [1–3]. miRNAs exhibit abnormal expression in many cancer types and affect the hallmarks of cancer, including sustaining proliferative signaling, evading growth suppressors, resisting cell death, inducing angiogenesis, activating invasion and metastasis, and avoiding immune destruction [4, 5]. Thus, manipulating the dysregulated miRNAs is a new therapeutic strategy for cancer [6]. Among the numerous cancer-associated miRNAs, the miR-124 family has received substantial attention, with three members (miR-124-1, miR-124-2, and miR-124-3) downregulated in many cancers [7, 8]. The tumor suppressive role of miR-124 is also evidenced by its target mRNA network, affecting the expression of oncoproteins such as K-Ras [9], epigenetic proteins such as EZH2 [10, 11], and transcript factors such as STAT3 [12–14]. Given that miR-124 targets a large pool of oncogenic mRNA, therapeutic strategies to replenish miR-124 may be of use in cancers.

Exosomes are nano-sized extracellular vesicles with a membrane lipid bilayer that play important roles in intercellular communication [15]. The biological function of exosomes is to deliver various effectors, such as lipids, metabolites, proteins, and nucleic acids, to target cells [16–19]. Accumulated evidence indicates that exosomes may serve as anticancer drug carriers to achieve targeted therapy [20–23]. For instance, mesenchymal stem cell (MSC)-derived exosomes suppress the growth of glioma, breast cancer, and pancreatic ductal adenocarcinoma both *in vitro* and *in vivo* by delivering miR-146b [24], miR-379 [25], miR-145-5p [26], or miR-124 [11], respectively. Exosomal let-7a derived from human embryonic kidney cell line 293 (HEK293) reduces breast cancer xenograft growth in a mouse model [27]. Upregulating miR-335-5p expression in stellate cell-derived exosomes can inhibit the growth and invasion of hepatocellular carcinoma cells in mice models [28]. Exosomes extracted from normal human foreskin fibroblasts can be engineered to deliver siRNA and shRNA constructs that target the $KRAS^{G12D}$ oncogene, these exosomes show significant inhibitory effects on pancreatic cancer models developed in immunocompromised and immunocompetent mice [29]. Taken together, controlling the expression of anti-tumor miRNAs using exosomes is of great significance in the treatment of tumors.

Metabolism reprogramming is thought to be a unique hallmark of tumor cells that sustains their uncontrolled growth and proliferation [30, 31]. This metabolic rewiring leads to glycolysis flux and lactate production [30, 31]. The tumor microenvironment (TME) enriched-lactate enables Treg cells to impair anti-cancer immunity, allowing cancer cells to evade immune destruction [32, 33]. In mammals, lactate's transport across biological membranes is mediated by MCTs of the solute carrier 16 (SLC16) family, which comprises14 genes in the human genome (i.e., *SLC16A1-A14*) [34]. Among them, MCT1 (SLC16A1), which Treg cells predominantly express, plays a critical role in lactate uptake and has recently emerged as a major and validated target in cancer therapy [32–34]. Genetic and pharmacological inhibition of MCT1 of Treg cells reduced the frequency of Treg cells and PD-1 expression by Treg cells in the TME and increased activated $CD8^+$ T cells, leading to significant inhibition of tumor growth by immunotherapy [32, 33].

Indeed, MCT1 has been demonstrated as a direct target of miR-124 [35–38]. Here, we showed that exosomal miR-124, derived from BM-MSCs, effectively targeted MCT1 of tumor-infiltrating Treg cells, thereby reversing anti-tumor immunity and improving PD-1 blockade therapy. These data open a new window for developing a miRNA-carried exosome therapy against lactate as cancer immunotherapy.

Materials and methods

Cell lines and cell culture. Ovarian cancer cell line ID8 (RRID: CVCL_VA22), was cultured in DMEM (C11995500BT, GIBCO) supplemented with penicillin G (100 U/mL) and streptomycin (100 mg/ml) (SV30010, Hyclone) and 10% fetal bovine serum (04-001-1ACS, BI). Bone marrow mesenchymal stromal cells (BM-MSCs) from C57BL/6 mice were purchased from Cyagen (MUBMX-01001). BM-MSCs were cultured in the MEM medium (C12571500CP, GIBCO) supplemented with penicillin G (100 U/ml) and streptomycin (100 mg/ml) (SV30010, Hyclone) and 10% fetal calf serum (04–001-1 ACS, BI). Cells were grown at 37°C in a humidified atmosphere with 5% CO_2.

Quantitative real-time polymerase chain reaction analysis. Total RNA of tissues and exosomes were extracted by TRIzol reagent (Invitrogen). After the determination of the RNA concentration, a PrimeScript™ RT reagent kit (TaKaRa, Dalian, China) was used to synthesize complementary DNA. Mature microRNAs in the sample were reverse transcribed to cDNA using TaqMan™ Advanced MicroRNA cDNA Synthesis Kit (Thermo Fisher, USA). qRT-PCR was performed using a SYBR Green Reagent (TaKaRa, Dalian, China). U6 was used to normalize microRNA. The $2^{-\Delta\Delta Ct}$ method was used to calculate the relative expression of genes. Each test was repeated 3 times. The primer sequences were as follows: mmu-miR-124-3p forward, 5'-TCTTTAAGGCACGCGGTG-3' and reverse 5'-TATGGTTTTGACGACTGTGTGAT-3'.

Transient miRNA transfection. miRNA-124-3p mimic (5'-UAAGGCACGCGGUGAAUGCC-3') and negative control (miR-NC) (5'-UUUGUACUACACAAAAGUACUG-3') were synthesized by Ribobio. BM-MSCs were transfected with miRNA-124-3p mimic or negative control using Lipofectamine® 3000 (Invitrogen; Thermo Fisher Scientific, Inc.), according to the manufacturer's protocol.

Cell isolation and flow cytometry. Tumor of mice was harvested and processed to signal cell suspensions of lymphocytes. Cells of interest were analyzed using surface markers, and for Foxp3, TNFα, or Ki-67 staining, surface marker-stained cells were fixed, permeabilized, and labeled with Foxp3-, TNFα-, or Ki-67-specific mAb. All flow cytometry data were captured using FASCcan Flow Cytometer and analyzed using the FlowJo software.

Exosome isolation and identification. Exosomes were prepared from BM-MSCs with miR-NC or miR-124-3p transfection. Briefly, the medium was collected and centrifuged at 1,000× g for 10 min at 4°C. Following centrifugation, the supernatant was passed through a 0.22 μm sterile filter (Steritop™ Millipore, MA, USA). Then, the filtered supernatant was performed for exosome isolation using a commercial kit (BIBOBIO, cat. no. C10130-1) according to the manufacturer's protocol. Western blotting was used to determine specific exosome surface markers, such as CD9 and CD63.

pHrodo red assay for lactic acid uptake. Cell suspensions from lymph nodes and mice tumors were loaded with pHrodo Red AM (ThermoFisher Scientific) according to the manufacturer's protocol in 20 mM HEPES in PBS. Cells were surface stained for multicolor flow cytometry following the normal protocol in 20 mM HEPES/PBS. At the flow cytometer, lactic acid was spiked into each sample at a final concentration of 5 mM (pH roughly 6.7). Samples were read at 30 min after the addition of lactic acid.

Exosome uptake by naïve $CD4^+$ T cells. The PKH-26-labeled exosomes were co-cultured with naïve $CD4^+$ T cells for 24 h. Then, the cells were washed with PBS and identified by flow cytometry.

Microsuppression and proliferation assays. Tumor-infiltrating Treg cells were isolated by flow-assisted sorting from tumors of C57BL/6J-$Foxp3^{GFP.cre}$ mice. $Foxp3^+$ iTregs were induced from naïve $CD4^+$ T cells. Briefly, naïve $CD4^+$ T cells were incubated for 3 days with CD3ε/CD28 mAb beads, plus TGF-β (3 ng/ml) and IL-2 (25 U/ml), and analyzed by flow cytometry for $Foxp3^+$ iTreg. For Treg cells suppression assays, Treg cells were co-cultured for 72 h with APCs and CellTrace™ Violet (CTV)-labeled $CD8^+$ T cells at ratios 1:5 in a complete RPMI medium with CD3ε mAb (1 μg/ml, Biolegend). Proliferation of $CD8^+$ T cells was determined by flow cytometric analysis of CellTrace Violet (CTV).

***In vivo* ovarian cancer xenograft model.** Animal protocols were approved by the animal care committee of Guangdong Provincial People's Hospital. ID8 cells (1×10^6) were

injected subcutaneously into the back of 4-week-old C57BL/6 female mice. Mice received intratumoral injection of miRNA or exosome after the tumors reached 5 mm in diameter. Tumor sizes were measured at the indicated times. Tumor volumes were estimated according to the following formula: volume = (longest diameter × shortest diameter^2)/2.

Western blot. Cells and exosomes were lysed in RIPA buffer containing protease and phosphatase inhibitors. Protein quantification was performed by BCA Protein Assay (Pierce; Thermo Fisher Scientific, Inc.). Then 20 μg of soluble protein were loaded onto each lane of 8–12% Bis-TRIS gel. The proteins were transferred to polyvinylidene fluoride (PVDF) membrane. For the immunoblot, the membranes were blocked with 5% skimmed milk (Bio-Rad Laboratories, Inc.) in TBST for 1 h. Primary antibodies (1:1000 dilution) in 5% bovine serum albumin (BSA) were added and incubated overnight at 4°C on a shaker. The membranes then were washed with TBST and incubated with a secondary antibody (1:5000 dilution) in 5% skimmed milk at room temperature for 1 h. The membranes then were washed with TBST and incubated with ECL mix (Epizyme; cat. no. SQ202). Rabbit antibody against MCT1 (cat. no. 20139-1-AP), CD9 (cat. no. 20597-1-AP), CD63 (cat. no. 25682-1-AP), mouse antibody against GAPDH (cat. no. 60004) and horseradish peroxidase-conjugated secondary antibodies (cat. no. SA00001-1 and SA00001-2) were obtained from ProteinTech Group, Inc.

Statistical analysis. The GraphPad Prism 7 was applied for statistical data analysis. Unpaired t-test was utilized to analyze the data conforming to normal distribution and homogeneity of variance between the two groups. All experiments were repeated 3 times unless stated otherwise. Data are presented as mean values with standard error of the mean (SEM). The two-sided p-value < 0.05 were defined as statistically significant.

Results

miR-124 impairs tumor infiltrating-Treg cells function. In the present study, miR-124 was detected in six pairs of primary ovarian cancer and corresponding healthy tissue. We found that miR-124 was downregulated in tumors (Figure 1A). Next, we evaluated *in vivo* miR-124's treatment effect on ovarian cancer using the xenograft C57BL/6 mice model (Figure 1B). Mice received an intratumoral injection of negative control (miR-NC) or miR-124-3p after the tumors reached 5 mm in diameter. Then, we examined the tumor infiltrating-Treg cells in NC- and miR-124-3p-treated groups by flow cytometry. Results showed that the proportion of Treg cells was reduced in miR-124-3p-treated infiltrates (Figure 1C). While characterization of intratumoral miR-124-3p-treated Treg cells revealed decreases in Ki-67, ICOS, and CD103 staining, as well as elevated PD-1 staining, potentially indicating dysfunctional Treg cells (Figures 1D–1G). To further identify miR-124-3p's tumor immune microenvironment (TIME) modulation in ovarian cancer, we measured the Treg cells suppressor activity, isolated from C57BL/6J-*Foxp3*^{GFPcre} mice bearing tumors, with NC or miR-124-3p treatment. By co-culturing CD8$^+$ T cells with Tregs^{NC} or Tregs$^{miR\text{-}124\text{-}3p}$, and using a CellTrace Violet (CTV) dilution assay as the readout for CD8$^+$ T cell proliferation. We found that Tregs$^{miR\text{-}124\text{-}3p}$ had reduced suppressive function *ex vivo* than Tregs^{NC} (Figure 1H). Also, increased numbers of TNF-α$^+$ CD8$^+$ T cells were found in Tregs$^{miR\text{-}124\text{-}3p}$ co-culture groups (Figure 1I). Collectively, these data suggested that miR-124-3p impaired functional tumor infiltrating-Treg cells.

miR-124 impairs Treg cells' function by reducing lactate uptake. Here, we found that miR-124 targeted MCT1 in naïve CD4$^+$ T cells (Figure 2A), which is in line with observations in tumor cells [36, 37, 39]. MCT1 functions in transporting lactate from the circulation into cells. Predictably, miR-124 dampened lactate uptake in naïve CD4$^+$ T cells (Figures 2B, 2C). We previously reported that lactate supported Treg cells' functions [40]. In the present study, naïve CD4$^+$ T cells were cultured under polarizing conditions to form iTregs. We observed an increase in iTreg formation, as well as suppressor activity, in the added Na L-lactate group (Figures 2D–2F). However, miR-124 transfection reversed Na L-lactate's effects (Figures 2D–2F). Altogether, these results suggested that miR-124 weakened lactate-induced Treg cells' polarization and function.

miR-124-carried exosomes impair Treg cells' function. Considering that exosomes may serve as miRNA carriers to achieve targeted therapy, we next investigated whether exosomes can be vehicles to deliver miR-124 into lymphocytes. The exosomes were prepared from miR-NC or miR-124-3p transfected BM-MSCs, and identified by CD9 and CD63 (Figures 3A, 3B). The expression level of miR-124 was much higher in Exo$^{miR\text{-}124\text{-}3p}$ than in Exo$^{miR\text{-}NC}$ (Figure 3C). The PKH-26 labeled exosomes were co-cultured with naïve CD4$^+$ T cells, flow cytometry analysis showed that both Exo$^{miR\text{-}NC}$ and Exo$^{miR\text{-}124\text{-}3p}$ could be engulfed by receptor cells (Figure 3D). In addition, Exo$^{miR\text{-}124\text{-}3p}$ led to a decrease in MCT1 expression in naïve CD4$^+$ T cells (Figure 3E). Next, naïve CD4$^+$ T cells were pre-treated with Exo$^{miR\text{-}NC}$ or Exo$^{miR\text{-}124\text{-}3p}$, and then were cultured under polarizing conditions to form iTregs. Compared to Exo$^{miR\text{-}NC}$, Exo$^{miR\text{-}124\text{-}3p}$ effectively suppressed iTreg formation and suppressor activity (Figures 3F–3H). All these results suggested that the exosomes could deliver miR-124 into Treg cells.

miR-124-carried exosomes impair tumor-infiltrating Treg cells' function and improve cancer immunotherapy. Lactic acid is highly enriched in the TME and is known to promote Treg-mediated suppression [32, 33, 40, 41]. To further investigate whether miR-124 could restrain Treg cells' lactate uptake *in vivo*, miR-NC or miR-124-3p was injected into tumors. The lactate uptake was subsequently analyzed in sorted tumor-infiltrating Treg cells (Figure 4A). Compared to miR-NC, miR-124-3p intratumoral injection reduced the lactate uptake in tumor-infiltrating Treg cells (Figure 4B).

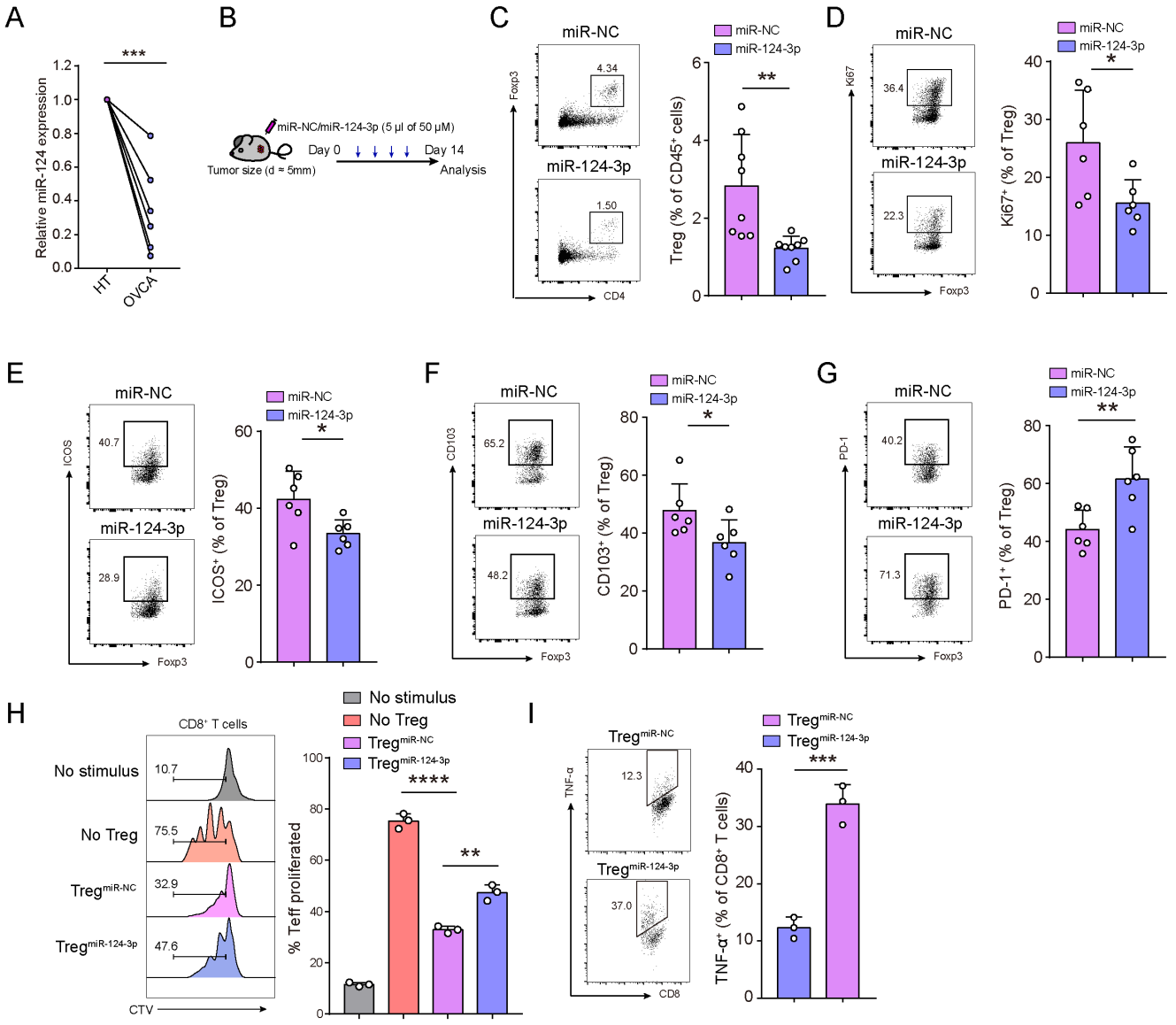

Figure 1. miR-124 impairs tumor-infiltrating Treg cells' function. A) Levels of miR-124 in six pairs of ovarian cancer and matched normal fallopian tube tissue. B) Tumoral injection of miR-NC or miR-124-3p. C) The proportion of tumor-infiltrating Treg cells was analyzed in miR-NC or miR-124-3p treated tumors. D) The expression of Ki-67 in tumor-infiltrating Treg cells was analyzed in miR-NC or miR-124-3p treated tumors. E) The expression of ICOS in tumor-infiltrating Treg cells was analyzed in miR-NC or miR-124-3p treated tumors. F) The expression of CD103 in tumor-infiltrating Treg cells was analyzed in miR-NC or miR-124-3p treated tumors. G) The expression of PD-1 in tumor-infiltrating Treg cells was analyzed in miR-NC or miR-124-3p treated tumors. H) Left, representative histogram showing the dilution of dye as a result of proliferation of $CD8^+$ T cells after 72 hours of co-culture with tumor-infiltrating Treg cells isolated from tumors of miR-NC- or miR-124-3p-treated C57BL/6J-*Foxp3*$^{GFP.cre}$ mice. Right, frequency of proliferated $CD8^+$ T cells co-culture with tumor-infiltrating Treg cells isolated from tumors of miR-NC- or miR-124-3p-treated C57BL/6J-*Foxp3*$^{GFP.cre}$ mice. I) Representative flow plot (left) and tabulated percentage (right) of TNF-α^+ $CD8^+$ T cells co-cultured with tumor-infiltrating Treg cells isolated from tumors of miR-NC- or miR-124-3p-treated C57BL/6J-*Foxp3*$^{GFP.cre}$ mice.

Similar results were also found in Exo$^{miR\text{-}124\text{-}3p}$ intratumoral injection (Figures 4C, 4D). Next, the sorted infiltrating-Treg cells underwent the suppression assays, results showed that intratumoral injection of Exo$^{miR\text{-}124\text{-}3p}$ significantly impaired infiltrating-Treg cells' suppressive capacity (Figures 4E, 4F). We next carried out a treatment study using ID8 xenograft in C57BL/6 mice. Results showed that anti-PD-1 monotherapy was able to reduce tumor size, a combination of Exo$^{miR\text{-}124\text{-}3p}$, but not Exo$^{miR\text{-}NC}$, and anti-PD-1 showed a greater reduction (Figure 4G). This enhancement in anti-tumor efficacy was also beneficial to survival, with combination therapy increasing survival more than either monotherapy (Figure 4H).

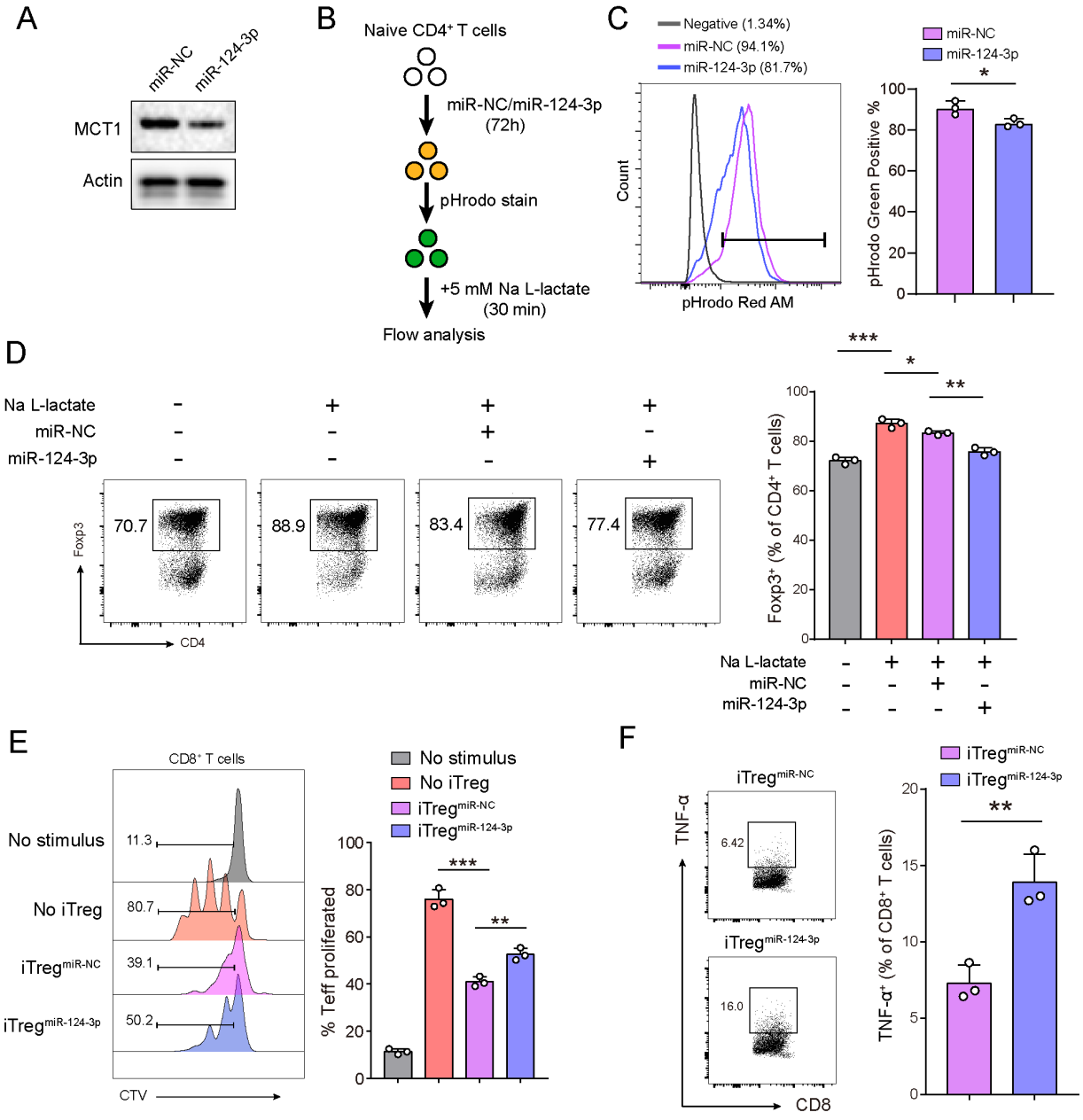

Figure 2. miR-124 impairs Treg cells' function by reducing lactate uptake. A) MCT1 expression in miR-NC and miR-124-3p transfected naïve CD4⁺ T cells was evaluated by western blot. B) Na L-lactate uptake was analyzed in miR-NC or miR-124-3p transfected naïve CD4⁺ T cells. C) Representative data (left) and quantified data (right) of Na L-lactate uptake in naïve CD4⁺ T cells with miR-NC or miR-124-3p transfection. D) Representative data (left) and quantified data (right) from Treg cells induction experiments with or without Na L-lactate treatment, miR-NC or miR-124-3p transfection. E) Left, representative histogram showing the dilution of dye as a result of the proliferation of CD8⁺ T cells after 72 h of co-culture with iTregs polarized with Na L-lactate treatment, miR-NC or miR-124-3p transfection. Right, frequency of proliferated CD8⁺ T cells co-culture with iTregs polarized with Na L-lactate treatment, miR-NC or miR-124-3p transfection. F) Representative flow plot (left) and tabulated percentage (right) of TNF-α⁺ CD8⁺ T cells co-cultured with iTregs polarized with Na L-lactate treatment, miR-NC or miR-124-3p transfection.

Discussion

Tumor cells are characterized by altered glucose metabolism known as the Warburg effect in which glycolysis flux and lactate production are increased [30, 31]. The lactate-rich TME is thought to support Treg cells' function through a distinct metabolic profile from other T cells [32, 33, 41]. Treg cells use lactate as a fuel and as a means to protect their high suppressive capacity, which leads to tumor immune evasion [32]. In addition, lactate uptake also induces PD-1

expression in Treg cells, and controls immune responses in the TME [33]. These observations suggest that controlling lactate uptake of Treg cells may be helpful to cancer therapy.

Owing to the important role of lactate in tumor development, inhibition of lactate metabolism by blocking monocarboxylate transporters becomes a potential strategy for tumor therapy [42, 43]. Early-developed MCTs inhibitors, such as phloretin and quercetin, are generally of low affinity and poor specificity [44, 45]. Recently, several more potent MCT1 inhibitors, such as AZD3965 and BAY-8002, have been reported with IC_{50} or K_i at nM range [46, 47]. ADZ3965 and BAY-8002 were reported to inhibit MCT1 and MCT2 but showed no effect on MCT4 [48]. Presently, AZD3965 is in phase I clinical trials. Indole derivatives, a new class of potent inhibitors of MCT1, also show functional inhibitory activities at low nM concentrations and great antiproliferative activities against the MCT1-expressing tumor cells, while they are selective over MCT4 [49].

Unlike the small-molecule inhibitors, miRNAs provide attractive and mechanistically different therapeutic strategies based on their potential for simultaneous modulation of multiple targets. miRNA-based therapeutic approaches against tumors have progressed from bench to bedside, with the development of delivery systems [1, 50, 51]. miR-34 mimic encapsulated in liposomes (MRX34) was evaluated in patients with advanced solid tumors (ClinicalTrials.gov identifier NCT01829971, NCT02862145). miR-16 mimic delivered in bacterial minicells coated with epidermal growth factor receptor (EGFR) antibody (MesomiR-1) was assessed in patients with malignant pleural mesothelioma or non-small-cell lung cancer (NSCLC) (ClinicalTrials.gov identifier NCT02369198). Currently, MSC-derived exosomes have attracted great research interest as a promising strategy to deliver therapeutic molecules including miRNAs and anti-miRNAs [52]. Unlike liposomes and other synthetic drug nanoparticle carriers, exosomes are released by all cells and contain transmembrane and membrane-anchored proteins, which enhance endocytosis and thus promote the transfer of their contents [53, 54]. In addition, exosomes express CD47, a 'don't eat me' signal that interacts with signal regulatory

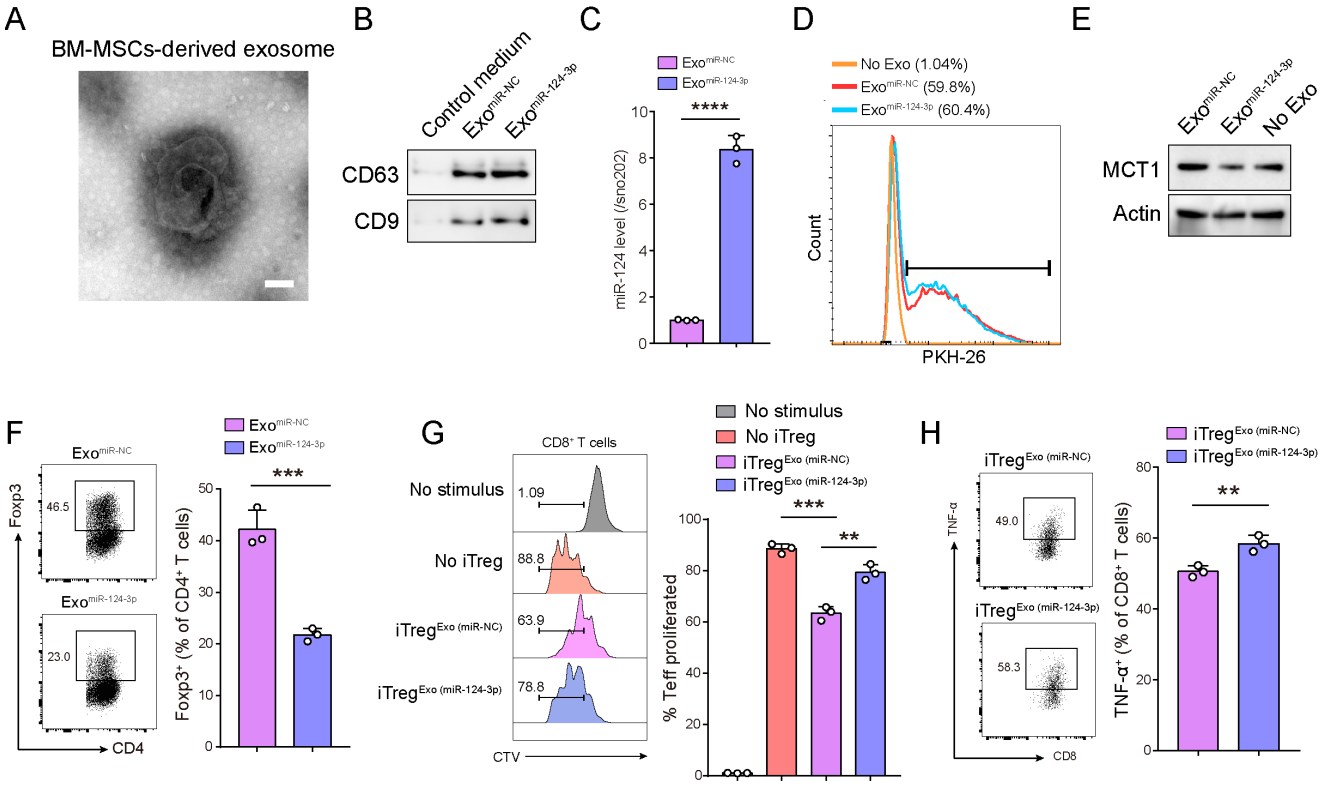

Figure 3. miR-124-carried exosomes impair Treg cell's function. A) TEM image of BM-MSC derived exosome. Scale bar, 100 nm B) CD9 and CD63 expressions in exosomes derived from miR-NC or miR-124-3p transfected BM-MSCs were evaluated by western blot. C) miR-124 expression in exosomes derived from miR-NC or miR-124-3p transfected BM-MSCs was evaluated by RT-qPCR. D) PKH-26 labeled exosomes derived from miR-NC or miR-124-3p transfected BM-MSCs were engulfed by naïve CD4+ T cells. E) MCT1 expression in exosome$^{miR\text{-}NC}$ or exosome$^{miR\text{-}124\text{-}3p}$ treated naïve CD4+ T cells was evaluated by western blot. F) Representative data (left) and quantified data (right) from Treg cells induction experiments with exosome$^{miR\text{-}NC}$ or exosome$^{miR\text{-}124\text{-}3p}$ treatment. G) Left, representative histogram showing the dilution of dye as a result of proliferation of CD8$^+$ T cells after 72 h of co-culture with iTregs polarized with exosome$^{miR\text{-}NC}$ or exosome$^{miR\text{-}124\text{-}3p}$ treatment. Right, frequency of proliferated CD8$^+$ T cells co-culture with iTregs polarized with exosome$^{miR\text{-}NC}$ or exosome$^{miR\text{-}124\text{-}3p}$ treatment. H) Representative flow plot (left) and tabulated percentage (right) of TNF-α$^+$ CD8$^+$ T cells co-cultured with iTregs polarized with exosome$^{miR\text{-}NC}$ or exosome$^{miR\text{-}124\text{-}3p}$ treatment.

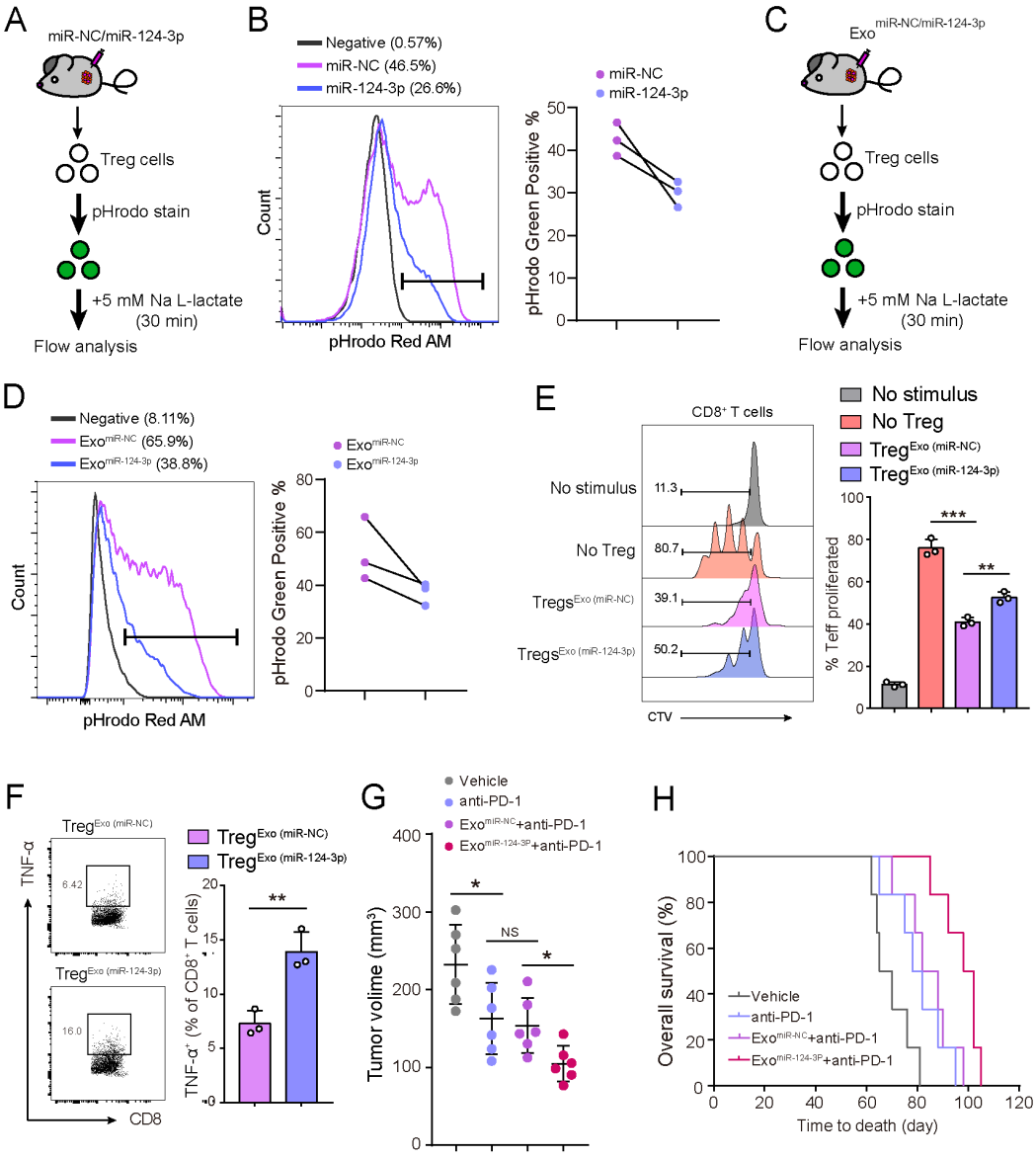

Figure 4. Exosomes-delivered miR-124 impairs tumor-infiltrating Treg cells' function and improves cancer immunotherapy. A) Na L-lactate uptake was analyzed in miR-NC or miR-124-3p treated tumor-infiltrating Treg cells. B) Representative data (left) and quantified data (right) of Na L-lactate uptake in tumor-infiltrating Treg cells isolated from tumors of miR-NC- or miR-124-3p-treated C57BL/6J-*Foxp3*$^{GFP.cre}$ mice. C) Na L-lactate uptake was analyzed in exosome$^{miR\text{-}NC}$ or exosome$^{miR\text{-}124\text{-}3p}$ treated tumor-infiltrating Treg cells. D) Representative data (left) and quantified data (right) of Na L-lactate uptake in tumor-infiltrating Treg cells isolated from tumors of exosome$^{miR\text{-}NC}$ or exosome$^{miR\text{-}124\text{-}3p}$ treated C57BL/6J-*Foxp3*$^{GFP.cre}$ mice. E) Left, representative histogram showing the dilution of dye as a result of proliferation of CD8$^+$ T cells after 72 hours of co-culture with tumor-infiltrating Treg cells isolated from tumors of exosome$^{miR\text{-}NC}$ or exosome$^{miR\text{-}124\text{-}3p}$ treated C57BL/6J-*Foxp3*$^{GFP.cre}$ mice. Right, frequency of proliferated CD8$^+$ T cells co-culture with tumor-infiltrating Treg cells isolated from tumors of exosome$^{miR\text{-}NC}$ or exosome$^{miR\text{-}124\text{-}3p}$ treated C57BL/6J-*Foxp3*$^{GFP.cre}$ mice. F) Representative flow plot (left) and tabulated percentage (right) of TNF-α$^+$ CD8$^+$ T cells co-cultured with tumor-infiltrating Treg cells isolated from tumors of exosome$^{miR\text{-}NC}$ or exosome$^{miR\text{-}124\text{-}3p}$ treated C57BL/6J-*Foxp3*$^{GFP.cre}$ mice. G) Treatment of ID8 tumors in C57BL/6 mice with exosome$^{miR\text{-}NC}$, exosome$^{miR\text{-}124\text{-}3p}$ and PD-1 blockade, and combination therapy. n=6, each group, experiment conducted once. Unpaired one-way ANOVA without multiple comparison correction. H) Survival analysis of mice shown in (G). n=6, each group, one-tailed log-rank Mantel-Cox test.

protein alpha (SIRPα) on circulating monocytes to prevent phagocytosis and thus increase half-life in the circulation [29]. However, several obstacles are urgently needed to overcome in the push toward a clinical routine application of exosomal miRNAs. The most critical issues to be addressed include the question of how to enable tissue-specific targeting, and what dose can achieve a therapeutic effect with minimal side effects. Collectively, our study offers insight into the therapeutic potential of BM-MSC-derived exosomal miR-124 in specific targeting of MCT1 of tumor-infiltrating Treg cells.

Acknowledgments: This work was supported by the Guangzhou Science and Technology Program Project [202102080046].

References

[1] HAYES J, PERUZZI PP, LAWLER S. MicroRNAs in cancer: biomarkers, functions and therapy. Trends Mol Med 2014; 20: 460–469. https://doi.org/10.1016/j.molmed.2014.06.005

[2] LIN S, GREGORY RI. MicroRNA biogenesis pathways in cancer. Nat Rev Cancer 2015; 15: 321–333. https://doi.org/10.1038/nrc3932

[3] HUSSEN BM, HIDAYAT HJ, SALIHI A, SABIR DK, TAHERI M et al. MicroRNA: A signature for cancer progression. Biomed Pharmacother 2021; 138: 111528. https://doi.org/10.1016/j.biopha.2021.111528

[4] HANAHAN, D. Hallmarks of Cancer: New Dimensions. Cancer Discov 2022; 12: 31–46. https://doi.org/10.1158/2159-8290.CD-21-1059

[5] PENG Y, CROCE CM. The role of MicroRNAs in human cancer. Signal Transduct Target Ther 2016; 1: 15004. https://doi.org/10.1038/sigtrans.2015.4

[6] RUPAIMOOLE R, SLACK FJ. MicroRNA therapeutics: towards a new era for the management of cancer and other diseases. Nat Rev Drug Discov 2017; 16: 203–222. https://doi.org/10.1038/nrd.2016.246

[7] GHAFOURI-FARD S, SHOOREI H, BAHROUDI Z, ABAK A, MAJIDPOOR J et al. An update on the role of miR-124 in the pathogenesis of human disorders. Biomed Pharmacother 2021; 135: 111198. https://doi.org/10.1016/j.biopha.2020.111198

[8] JIA X, WANG X, GUO X, JI J, LOU G et al. MicroRNA-124: An emerging therapeutic target in cancer. Cancer Med 2019; 8: 5638–5650. https://doi.org/10.1002/cam4.2489

[9] JIN H, LI Q, CAO F, WANG SN, WANG RT et al. miR-124 Inhibits Lung Tumorigenesis Induced by K-ras Mutation and NNK. Mol Ther Nucleic Acids 2017: 9: 145–154. https://doi.org/10.1016/j.omtn.2017.09.005

[10] SONG BF, XU LZ, JIANG K, CHENG F. MiR-124-3p inhibits tumor progression in prostate cancer by targeting EZH2. Funct Integr Genomics 2023; 23: 80. https://doi.org/10.1007/s10142-023-00991-8

[11] XU Y, LIU N, WEI Y, ZHOU D, LIN R et al. Anticancer effects of miR-124 delivered by BM-MSC derived exosomes on cell proliferation, epithelial mesenchymal transition, and chemotherapy sensitivity of pancreatic cancer cells. Aging (Albany NY) 2020; 12: 19660–19676. https://doi.org/10.18632/aging.103997

[12] WEI J, WANG F, KONG LY, XU S, DOUCETTE T et al. miR-124 inhibits STAT3 signaling to enhance T cell-mediated immune clearance of glioma. Cancer Res 2013; 73: 3913–3926. https://doi.org/10.1158/0008-5472.CAN-12-4318

[13] KOUKOS G, POLYTARCHOU C, KAPLAN JL, MORLEY-FLETCHER A, GRAS-MIRALLES B et al. MicroRNA-124 regulates STAT3 expression and is down-regulated in colon tissues of pediatric patients with ulcerative colitis. Gastroenterology 2013; 145: 842–52.e2. https://doi.org/10.1053/j.gastro.2013.07.001

[14] LIN S, LIU Q, WEN J, BAI K, GUO Y et al. Mir-124 Attenuates STAT3-Mediated TH17 Differentiation in Colitis-Driven Colon Cancer. Front Oncol 2020; 10: 570128. https://doi.org/10.3389/fonc.2020.570128

[15] KALLURI R, LEBLEU VS. The biology, function, and biomedical applications of exosomes. Science 2020; 367: eaau6977. https://doi.org/10.1126/science.aau6977

[16] SKOTLAND T, SANDVIG K, LLORENTE A. Lipids in exosomes: Current knowledge and the way forward. Prog Lipid Res 2017; 66: 30–41. https://doi.org/10.1016/j.plipres.2017.03.001

[17] PUHKA M, TAKATALO M, NORDBERG ME, VALKONEN S, NANDANIA J et al. Metabolomic Profiling of Extracellular Vesicles and Alternative Normalization Methods Reveal Enriched Metabolites and Strategies to Study Prostate Cancer-Related Changes. Theranostics 2017; 7: 3824–3841. https://doi.org/10.7150/thno.19890

[18] SCHEY KL, LUTHER JM, ROSE KL. Proteomics characterization of exosome cargo. Methods 2015: 87: 75–82. https://doi.org/10.1016/j.ymeth.2015.03.018

[19] VAN DEN BOORN JG, DASSLER J, COCH C, SCHLEE M, HARTMANN G. Exosomes as nucleic acid nanocarriers. Adv Drug Deliv Rev 2013; 65: 331–335. https://doi.org/10.1016/j.addr.2012.06.011

[20] DAI J, SU Y, ZHONG S, CONG L, LIU B et al. Exosomes: key players in cancer and potential therapeutic strategy. Signal Transduct Target Ther 2020; 5: 145. https://doi.org/10.1038/s41392-020-00261-0

[21] WANG X, TIAN L, LU J, NG IO. Exosomes and cancer – Diagnostic and prognostic biomarkers and therapeutic vehicle. Oncogenesis 2022; 11: 54. https://doi.org/10.1038/s41389-022-00431-5

[22] RAGURAMAN R, BHAVSAR D, KIM D, REN X, SIKAVITSAS V et al. Tumor-targeted exosomes for delivery of anticancer drugs. Cancer Lett 2023: 558: 216093. https://doi.org/10.1016/j.canlet.2023.216093

[23] SYN NL, WANG L, CHOW EK, LIM CT, GOH BC. Exosomes in Cancer Nanomedicine and Immunotherapy: Prospects and Challenges. Trends Biotechnol 2017; 35: 665–676. https://doi.org/10.1016/j.tibtech.2017.03.004

[24] KATAKOWSKI M, BULLER B, ZHENG X, LU Y, ROGERS T et al. Exosomes from marrow stromal cells expressing miR-146b inhibit glioma growth. Cancer Lett 2013; 335: 201–204. https://doi.org/10.1016/j.canlet.2013.02.019

[25] O'BRIEN KP, KHAN S, GILLIGAN KE, ZAFAR H, LALOR P et al. Employing mesenchymal stem cells to support tumor-targeted delivery of extracellular vesicle (EV)-encapsulated microRNA-379. Oncogene 2018; 37: 2137–2149. https://doi.org/10.1038/s41388-017-0116-9

[26] DING Y, CAO F, SUN H, WANG Y, LIU S et al. Exosomes derived from human umbilical cord mesenchymal stromal cells deliver exogenous miR-145-5p to inhibit pancreatic ductal adenocarcinoma progression. Cancer Lett 2019; 442: 351–361. https://doi.org/10.1016/j.canlet.2018.10.039

[27] OHNO SI, TAKANASHI M, SUDO K, UEDA S, ISHIKAWA A et al. Systemically injected exosomes targeted to EGFR deliver antitumor microRNA to breast cancer cells. Mol Ther 2013; 21: 185–191. https://doi.org/10.1038/mt.2012.180

[28] WANG F, LI L, PIONTEK K, SAKAGUCHI M, SELARU FM. Exosome miR-335 as a novel therapeutic strategy in hepatocellular carcinoma. Hepatology 2018; 67: 940–954. https://doi.org/10.1002/hep.29586
[29] KAMERKAR S, LEBLEU VS, SUGIMOTO H, YANG S, RUIVO CF et al. Exosomes facilitate therapeutic targeting of oncogenic KRAS in pancreatic cancer. Nature 2017; 546: 498–503. https://doi.org/10.1038/nature22341
[30] FAUBERT B, SOLMONSON A, DEBERARDINIS RJ. Metabolic reprogramming and cancer progression. Science 2020; 368: eaaw5473. https://doi.org/10.1126/science.aaw5473
[31] MARTINEZ-REYES I, CHANDEL NS. Cancer metabolism: looking forward. Nat Rev Cancer 2021; 21: 669–680. https://doi.org/10.1038/s41568-021-00378-6
[32] WATSON MJ, VIGNALI PDA, MULLETT SJ, OVERACRE-DELGOFFE AE, PERALTA RM et al. Metabolic support of tumour-infiltrating regulatory T cells by lactic acid. Nature 2021; 591: 645–651. https://doi.org/10.1038/s41586-020-03045-2
[33] KUMAGAI S, KOYAMA S, ITAHASHI K, TANEGASHIMA T, LIN YT et al. Lactic acid promotes PD-1 expression in regulatory T cells in highly glycolytic tumor microenvironments. Cancer Cell 2022; 40: 201–218.e9. https://doi.org/10.1016/j.ccell.2022.01.001
[34] BOSSHART PD, CHARLES RP, GARIBSINGH RA, SCHLESSINGER A, FOTIADIS D. SLC16 Family: From Atomic Structure to Human Disease. Trends Biochem Sci 2021; 46: 28–40. https://doi.org/10.1016/j.tibs.2020.07.005
[35] WU DH, LIANG H, LU SN, WANG H, SU ZL et al. miR-124 Suppresses Pancreatic Ductal Adenocarcinoma Growth by Regulating Monocarboxylate Transporter 1-Mediated Cancer Lactate Metabolism. Cell Physiol Biochem 2018; 50: 924–935. https://doi.org/10.1159/000494477
[36] XU SY, JIANG XL, LIU Q, XU J, HUANG J et al. Role of rno-miR-124-3p in regulating MCT1 expression in rat brain after permanent focal cerebral ischemia. Genes Dis 2019; 6: 398–406. https://doi.org/10.1016/j.gendis.2019.01.002
[37] HOU L, ZHAO Y, SONG GQ, MA YH, JIN XH et al. Interfering cellular lactate homeostasis overcomes Taxol resistance of breast cancer cells through the microRNA-124-mediated lactate transporter (MCT1) inhibition. Cancer Cell Int 2019; 19: 193. https://doi.org/10.1186/s12935-019-0904-0
[38] LI KKW, PANG JCS, CHING AKK, WONG CK, KONG X et al. miR-124 is frequently down-regulated in medulloblastoma and is a negative regulator of SLC16A1. Hum Pathol 2009; 40: 1234–1243. https://doi.org/10.1016/j.humpath.2009.02.003
[39] YI C, YU AM. MicroRNAs in the Regulation of Solute Carrier Proteins Behind Xenobiotic and Nutrient Transport in Cells. Front Mol Biosci 2022; 9: 893846. https://doi.org/10.3389/fmolb.2022.893846
[40] CHEN J, HUANG ST, CHEN JG, HE JH, LIN WM et al. Resveratrol reduces lactate production and modifies the ovarian cancer immune microenvironment. Neoplasma 2022; 69: 1129–1137. https://doi.org/10.4149/neo_2022_220414N410
[41] ANGELIN A, GIL-DE-GÓMEZ L, DAHIYA S, JIAO J, GUO L et al. Foxp3 Reprograms T Cell Metabolism to Function in Low-Glucose, High-Lactate Environments. Cell Metab 2017; 25: 1282–1293.e7. https://doi.org/10.1016/j.cmet.2016.12.018
[42] DOHERTY JR, CLEVELAND JL. Targeting lactate metabolism for cancer therapeutics. J Clin Invest 2013; 123: 3685–3692. https://doi.org/10.1172/JCI69741
[43] PURI S, JUVALE K. Monocarboxylate transporter 1 and 4 inhibitors as potential therapeutics for treating solid tumours: A review with structure-activity relationship insights. Eur J Med Chem 2020; 199: 112393. https://doi.org/10.1016/j.ejmech.2020.112393
[44] PÉREZ-ESCUREDO J, VAN HÉE VF, SBOARINA M, FALCES J, PAYEN VL et al. Monocarboxylate transporters in the brain and in cancer. Biochim Biophys Acta 2016; 1863: 2481–2497. https://doi.org/10.1016/j.bbamcr.2016.03.013
[45] Park SJ, Smith CP, Wilbur RR, Cain CP, Kallu SR et al. An overview of MCT1 and MCT4 in GBM: small molecule transporters with large implications. Am J Cancer Res 2018; 8: 1967–1976.
[46] Ovens MJ, Davies AJ, Wilson MC, Murray CM, Halestrap AP. AR-C155858 is a potent inhibitor of monocarboxylate transporters MCT1 and MCT2 that binds to an intracellular site involving transmembrane helices 7-10. Biochem J 2010; 425: 523–530. https://doi.org/10.1042/BJ20091515
[47] QUANZ M, BENDER E, KOPITZ C, GRÜNEWALD S, SCHLICKER A et al. Preclinical Efficacy of the Novel Monocarboxylate Transporter 1 Inhibitor BAY-8002 and Associated Markers of Resistance. Mol Cancer Ther 2018; 17: 2285–2296. https://doi.org/10.1158/1535-7163.MCT-17-1253
[48] PAYEN VL, MINA E, VAN HEE VF, PORPORATO PE, SONVEAUX P. Monocarboxylate transporters in cancer. Mol Metab 2020; 33: 48–66. https://doi.org/10.1016/j.molmet.2019.07.006
[49] PURI S, STEFAN K, KHAN SL, PAHNKE J, STEFAN SM et al. Indole Derivatives as New Structural Class of Potent and Antiproliferative Inhibitors of Monocarboxylate Transporter 1 (MCT1; SLC16A1). J Med Chem 2023; 66: 657–676. https://doi.org/10.1021/acs.jmedchem.2c01612
[50] DIENER C, KELLER A, MEESE E. Emerging concepts of miRNA therapeutics: from cells to clinic. Trends Genet 2022; 38: 613–626. https://doi.org/10.1016/j.tig.2022.02.006
[51] FUERTES T, RAMIRO AR, DE YEBENES VG. miRNA-Based Therapies in B Cell Non-Hodgkin Lymphoma. Trends Immunol 2020; 41: 932–947. https://doi.org/10.1016/j.it.2020.08.006
[52] LAI RC, CHEN TS, LIM SK. Mesenchymal stem cell exosome: a novel stem cell-based therapy for cardiovascular disease. Regen Med 2011; 6: 481–492. https://doi.org/10.2217/rme.11.35
[53] JOHNSEN KB, GUDBERGSSON JM, NAJBJERG SKOV M, PILGAARD L, MOOS T et al. A comprehensive overview of exosomes as drug delivery vehicles – endogenous nanocarriers for targeted cancer therapy. Biochim Biophys Acta 2014; 1846: 75–87. https://doi.org/10.1016/j.bbcan.2014.04.005
[54] VADER P, MOL EA, PASTERKAMP G, SCHIFFELERS RM. Extracellular vesicles for drug delivery. Adv Drug Deliv Rev 2016; 106: 148–156. https://doi.org/10.1016/j.addr.2016.02.006